Frontiers in Bioscience Landmark

Front. Biosci. (Landmark Ed) **2024**; 29(9): 326
https://doi.org/10.31083/j.fbl2909326

Original Research

Multilayer Gelatin-Supported BMP-9 Coating Promotes Osteointegration and Neo-Bone Formation at the n-CDHA/PAA Composite Biomaterial-Bone Interface

Qiming Yang[1,†], Yue Li[2,†], Ruijie Wan[1], Lujue Dong[1], An He[3], Deyu Zuo[4,5,*], Zhenyu Dai[1,*]

[1]Department of Orthopedics, Chongqing Traditional Chinese Medicine Hospital, 400021 Chongqing, China
[2]Department of Clinical Laboratory, the Second Affiliated Hospital, Chongqing Medical University, 400000 Chongqing, China
[3]Division of Cardiology, The First Affiliated Hospital of Chongqing Medical University, 400016 Chongqing, China
[4]Department of Rehabilitation Medicine, The First Affiliated Hospital of Chongqing University of Chinese Medicine, Chongqing Traditional Chinese Medicine Hospital, 400021 Chongqing, China
[5]Chongqing Precision Medical Industry Technology Research Institute, 400000 Chongqing, China
*Correspondence: qmuzuodeyu@163.com (Deyu Zuo); zhenyudai1234@163.com (Zhenyu Dai)
[†]These authors contributed equally.

Academic Editor: Viviana di Giacomo
Submitted: 15 July 2024 Revised: 22 August 2024 Accepted: 26 August 2024 Published: 20 September 2024

Abstract

Background: The development of biomaterials capable of accelerating bone wound repair is a critical focus in bone tissue engineering. This study aims to evaluate the osteointegration and bone regeneration potential of a novel multilayer gelatin-supported Bone Morphogenetic Protein 9 (BMP-9) coated nano-calcium-deficient hydroxyapatite/poly-amino acid (n-CDHA/PAA) composite biomaterials, focusing on the material-bone interface, and putting forward a new direction for the research on the interface between the coating material and bone. **Methods**: The BMP-9 recombinant adenovirus (Adenovirus (Ad)-BMP-9/Bone Marrow Mesenchymal Stem Cells (BMSc)) was produced by transfecting BMSc and supported using gelatin (Ad-BMP-9/BMSc/Gelatin (GT). Multilayer Ad-BMP-9/BMSc/GT coated nano-calcium deficient hydroxyapatite/polyamino acid (n-CDHA/PAA) composite biomaterials were then prepared and co-cultured with MG63 cells for 10 days, with biocompatibility assessed through microscopy, Cell Counting Kit-8 (CCK-8), and alkaline phosphatase (ALP) assays. Subsequently, multilayer Ad-BMP-9/BMSc/GT coated n-CDHA/PAA composite biomaterial screws were fabricated, and the adhesion of the coating to the substrate was observed using scanning electron microscopy (SEM). *In vivo* studies were conducted using a New Zealand White rabbit intercondylar femoral fracture model. The experimental group was fixed with screws featuring multilayer Ad-BMP-9/BMSc/GT coatings, while the control groups used medical metal screws and n-CDHA/PAA composite biomaterial screws. Fracture healing was monitored at 1, 4, 12, and 24 weeks, respectively, using X-ray observation, Micro-CT imaging, and SEM. Integration at the material-bone interface and the condition of neo-tissue were assessed through these imaging techniques. **Results**: The Ad-BMP-9/GT coating significantly enhanced MG63 cell adhesion, proliferation, and differentiation, while increasing BMP-9 expression *in vitro*. *In vivo* studies using a rabbit femoral fracture model confirmed the biocompatibility and osteointegration potential of the multilayer Ad-BMP-9/BMSc/GT coated n-CDHA/PAA composite biomaterial screws. Compared to control groups (medical metal screws and n-CDHA/PAA composite biomaterial screws), this material demonstrated faster fracture healing, stronger osteointegration, and facilitated new bone tissue formation with increased calcium deposition at the material-bone interface. **Conclusion**: The multilayer GT-supported BMP-9 coated n-CDHA/PAA composite biomaterials have demonstrated favorable osteogenic cell interface performance, both *in vitro* and *in vivo*. This study provides a foundation for developing innovative bone repair materials, holding promise for significant advancements in clinical applications.

Keywords: bone tissue engineering; composite biomaterial; gelatin-supported BMP-9 coating; n-CDHA/PAA

1. Introduction

Medical metallic biomaterials have become the main choice for clinical fracture internal fixation treatment worldwide because of their high mechanical strength and biological inertness. However, due to its shortcomings such as masking effect, metal electrolytic corrosion, easy fatigue, imaging interference, poor histocompatibility, and the need for secondary surgical removal, non-metallic biomaterials have become another alternative for clinical internal fixation of fractures. Compared with metallic biomaterials, non-metallic biomaterials have lower modulus of elasticity, better biocompatibility and biodegradation properties. The interface between the biomaterial and the host bone is often the key to the success of internal fixation surgery. Ideal osseointegration requires that the bone tissue can be deposited directly on the implant surface, and that the implant is chemically bonded to the bone tissue rather than being in physical contact only, and that the implant can be long-lastingly and sufficiently biomechanically stabilized. However, the vast majority of non-metallic biomaterials studied

so far only have good osteoconductive properties and insufficient osteoinductive function. In recent years, the modification of non-metallic biomaterials with surface coatings has been beneficial in promoting the formation of chemical bonding between the material and the host bone, improving the osteointegration interface condition [1]. Therefore, surface coating of nonmetallic biomaterials to make them have good osteoinductive function, so as to obtain a good material-bone interface is one of the focuses of current research on the application of nonmetallic biomaterials.

Surface coating technology, i.e., increasing the physical and chemical properties of the implant surface by certain technical means, is used to change the surface of the implant that is in direct contact with the bone tissue after implant placement, thus promoting faster and better osseointegration of the implant with the bone tissue surface or giving the implant a better biologically active function [2]. Surface coatings have been shown to significantly enhance the functional properties of hip and knee prostheses, improving hardness, wettability, elastic strain, coefficient of friction, and wear resistance [3,4]. Among these, polyethylene coatings on non-biological material are currently the most prevalent in orthopedic clinics [5,6]. Extensive research has been conducted on coatings for joint replacement applications, utilizing materials such as diamond-like carbon, graphite-like carbon, tantalum, and titanium nitride. These coatings have been fabricated using various techniques, including physical or chemical vapor deposition, electrodeposition, molten salt heat treatment, laser shaping, and ion implantation. It has shown that the wear rate of ceramic materials is much less than that of polyethylene, and the wear of carbon coatings is several times less than that of ceramic materials [7]. Diamond-like, graphite-like, and tantalum-coated surfaces have proven to exhibit superior mechanical properties, including reduced surface roughness, increased hardness, and improved elastic strain. These coatings also demonstrate enhanced tribological performance, resulting in lower wear rate [4]. Nevertheless, research on these nonmetallic biomaterials has mainly focused on the improvement of physical properties such as coefficient of friction, yet very little research has been conducted on the material-bone interface. Therefore, it is important to develop a surface coating that releases bioactive factors for nonmetallic biomaterials to promote their osteointegration at the interface with bone.

Bioactive factors are a class of peptides that selectively bind to specific, high-affinity cell membrane receptors, triggering a cascade of effects that regulate cell growth and other cellular processes. Currently, bioactive factors that promote new bone production are mainly focused on vascular endothelial growth factor, matrix metalloproteinase family, transforming growth factor and bone morphogenetic proteins (BMPs) [8]. Among them, BMPs are a class of biologically active proteins isolated from bone matrix, which are capable of inducing the differentiation of undifferentiated and differentiated stem cells into chondrocytes, osteoblasts, and osteoclast precursor cells to promote bone production [9,10]. A study of 14 BMPs showed that five of them (2, 4, 6, 7, and 9) possessed potent osteogenic activity, and BMP-9 was found to have the strongest osteogenic activity [11]. Existing studies have reported that BMP-9 promotes stem cell osteogenic differentiation through various mechanisms [12], such as activating the phosphorylation of the transcription factor Smad1/5/8 to regulate the expression of downstream genes and inducing stem cell osteogenic differentiation [13]; inducing the expression of Hey1 to promote Mesenchymal Stem Cells (MSCs) osteogenesis [14]; interacting with the Notch signaling pathway to induce embryonic fibroblastic stem cells to become bone [15]; and up-regulating the up-regulation of long non-coding RNA (lncRNA) H19 induces early osteogenesis in MSCs [15]. Together, these studies suggest that BMP-9 has a role in promoting osteogenic differentiation of stem cells *in vitro* and *in vivo*, and also imply that we BMP-9 may promote fracture healing. Localized release of exogenous growth factors to promote tissue rejuvenation is an effective means of regenerative repair; however, as with other growth factors, BMP-9-coated pro-osteogenic release still suffers from uncontrollable flow, uneven distribution, abrupt release, and over piggybacking at a threshold level to maintain osteoblast proliferation and differentiation. As such, piggybacking for ordered release of the growth factor is critical.

In situ polymerization-derived nano-calcium deficient hydroxyapatite/polyamino acid (n-CDHA/PAA) is a degradable non-metallic biocomposite material. Previous study has shown that it possesses excellent biocompatibility, biomechanics, and biodegradability [16]. To evaluate its potential for internal fixation, we fabricated n-CDHA/PAA composite bio-screws and tested their efficacy in a rabbit intercondylar fracture model. Our findings revealed comparable fixation efficacy of n-CDHA/PAA bioactive screws to metallic screws, along with superior tissue compatibility. However, a significantly lower pull-out strength was observed for n-CDHA/PAA screws within the initial 4 weeks of fixation, potentially compromising internal fixation stability. Observations via SEM and immunohistochemistry revealed that this was likely due to the predominantly mechanical interlocking between the screw threads and bone tissue at the interface, lacking sufficient osteointegration strength. Enhancing the initial integration of the n-CDHA/PAA screws with bone tissue at the interface is an effective approach to mitigate this issue.

In summary, the present study was designed to design a multilayer Gelatin (GT) membrane carrying BMP-9 coating on homemade n-CDHA/PAA composite biomaterial screws, and to study the ordered release of BMP-9 biologic factors, the initial internal fixation strength, and the interface between the bio-screw material and the bone of the coated screws through *in vivo* and *ex vivo* experiments.

It lays a solid theoretical and practical foundation for the future research on the interface between the coated material and bone.

2. Materials and Methods

2.1 BMP-9 Expression Recombinant Adenovirus Preparation

Bone Marrow Mesenchymal Stem Cells (BMSc) primary cells (HUM-iCell-s011, iCell Bioscience, Shanghai, China) were passed the mycoplasma and Short Tandem Repeat (STR) certification, then cultured, passaged and frozen in liquid nitrogen for spare parts to obtain the appropriate titer of Flag-tagged BMP-9 recombinant adenovirus for transfection of BMSc cells, and Flag-tagged BMP-9 recombinant adenovirus (Ad-BMP-9) was used to transfect BMSc cells.

2.2 BMSc Cell Grouping

Cells in good growth status, after reaching 80% density, were washed with Phosphate Buffered Saline (PBS) (10010002, Gibco™, Waltham, MA, USA) in culture flasks, added with 0.25% trypsin digest, incubated at 37 °C for 2 minutes, gently shaken to dislodge all cells, centrifuged by adding 3 mL of medium, discarded the supernatant, and blown up into cell suspension. Subsequently, the cells were counted on a hemocyte counting plate, and the cell density was adjusted to 2×10^5 cells/mL for spreading.

The cells were grouped after attaching to the wall. (1) Ad-vector: the cell fusion rate reached about 50%, change fresh medium 1h in advance, use empty adenovirus, infect the cells with 20 µL of adenovirus in T25 cell bottles for 48 hours, and observe the cells under the microscope after the change of the solution; (2) Overexpression group (Ad-BMP9): the cell fusion rate reached about 50%, change fresh medium 1h in advance, use Flag-tagged BMP-9 adenovirus to infect one T25 cell bottle with 20 µL for 48 hours, and observe the cells under the microscope (BLD-200, COSSIM, Beijing, China).

2.3 Ad-BMP-9/BMSc/GT Preparation and Detection

BMSc cells that had been transfected with Ad-BMP-9 were taken to spread 80% of the bottom of the dish and centrifuged after trypsin termination. Remove the supernatant, add complete medium to resuspend, and adjust the cell concentration to 2×10^6 cells/mL. 3 mL of liquid GT (G0040, Solarbio, China) was taken in a 6-well plate, and aspirate 2 mL of the above Ad-BMP-9/BMSc cell suspension slowly and dropwise added to liquid GT to make Ad-BMP-9/BMSc/GT, and set aside.

MG63 cells (CRL-1427, ATCC, Manassas, VA, USA) were authenticated by STR profiling and confirmed to be free of mycoplasma contamination. Cells were harvested by trypsin digestion, counted, and adjusted to a density of 2×10^5 cells/mL. Ad-BMP-9/BMSc/GT was then co-cultured with MG63 cells for 10 days.

Group culture: (1) Ad-vector/BMSc/GT+MG63 cell co-culture control group; (2) Ad-BMP-9/BMSc/GT+MG63 cell co-culture group. GT was used as the control, and the proliferation and differentiation of Ad-BMP-9/BMSc/GT-promoted osteoblasts were observed by inverted biomicroscope (CKX3-SLP, OLYMPUS, Japan) morphology observation, Cell Counting Kit-8 (CCK-8), and human alkaline phosphatase (ALP) activity assay on the 1st, 5th, and 10th days, respectively.

2.4 Biocompatibility Analysis of Multilayer Ad-BMP-9/BMSc/GT Coated n-CDHA/PAA Composite Biomaterials in Vitro

The n-CDHA/PAA composite biomaterial discs with 30% n-CDHA mass ratio were prepared by *in situ* polymerization method, and the size of the discs was $\varphi 6 \times 2$ mm. n-CDHA/PAA composite biomaterials with multilayers of Ad-BMP-9/BMSc/GT coating were prepared as follows. Step 1: Ad-BMP-9/BMSc cell suspension with a cell concentration of 2×10^6 cells/mL was taken and slowly added dropwise to the surface of n-CDHA/PAA discs after freeze-drying using liquid nitrogen (first layer coating); Step 2: Liquid GT with a thickness of about 1 mm was coated on the first layer coating after freeze-drying using liquid nitrogen (second layer coating); Step 3: The first and second steps above were repeated to make the multilayer Ad-BMP-9/BMSc/GT coated n-CDHA/PAA composite biomaterial.

According to the experimental design the following three experimental subgroups were designed: (1) n-CDHA/PAA control group (without any coating treatment); (2) control group of composite biomaterials of n-CDHA/PAA with single-layer coated GT; and (3) experimental group of composite biomaterials of multilayered Ad-BMP-9/BMSc/GT coated n-CDHA/PAA. After co-culturing the materials of the experimental and control groups with well-grown MG63 cells for 10 days, the cell culture medium was aspirated at day 1, 5, and 10, respectively, followed by two washes with PBS. According to the protocols of the Cell Plasma Membrane Staining Kit with DiO (Green Fluorescence) (C1993S, Beyotime, Shanghai, China), an appropriate volume of green fluorescent cell membrane staining working solution was added and gently agitated to ensure uniform staining of all cells. The cells were incubated at 37 °C in the dark for 20 minutes. The cell membrane staining working solution was then aspirated, and the cells were washed three times with PBS. Finally, 37 °C pre-warmed cell culture medium was added, and the adhesion and growth of MG63 cells on the material surface were observed under an inverted biological microscope. The proliferation of MG63 cells and ALP activity were observed by CCK-8 and ALP activity analysis at three time points, respectively; and the proliferation of MG63 cells and the activity of ALP were detected by Quantitative Polymerase Chain Reaction (q-PCR) and Western Blot (WB), respectively, in the MG63 cells.

2.5 CCK-8 Assay

Cell proliferation of MG63 cells was assessed using a CCK-8 assay (C0038, Beyotime, China) at three time points (days 1, 5, and 10). Cells were seeded in 96-well plates, and 10 µL of CCK-8 solution was added into each well. Blank wells containing only cell culture medium and CCK-8 solution were used as zero controls. Plates were incubated in a cell culture incubator (BPH-9042, Yiheng, Shanghai) for 1 hour. Absorbance was measured at 450 nm using an enzyme marker (CMax Plus, Molecular Devices, San Jose, CA, USA).

2.6 Human Alkaline Phosphatase (ALP) Activity Analysis

Following the procedure described in the manual, the ALP enzyme-linked immunosorbent assay (ELISA) kit (CB12388-Hu, COIBO, Shanghai, China) was used to perform cell activity analysis of MG63 cells at three different time points (Day 1, Day 5, and Day 10). The cell suspension was diluted with phosphate-buffered saline (PBS). Cells were lysed and intracellular components were released through repeated freezing and thawing. After centrifugation for 20 minutes, the supernatant was collected. Standard wells, sample wells, and blank wells were set up accordingly. A standard curve was generated using different concentrations of the standard in the standard wells. Sample wells were loaded with 10 µL of cell lysate, followed by the addition of 100 µL of the enzyme-labeled reagent. After incubation at 37 °C for 60 minutes, the wells were washed five times with diluted washing solution. The chromogenic agent was added, and color development was allowed proceed in the dark at 37 °C for 15 minutes. Following reaction termination, the absorbance (OD value) was measured at 450 nm using an enzyme-linked immunosorbent assay reader (CMax Plus, Molecular Devices, USA).

2.7 Western Blotting

Cell lysates were prepared from each group using Radioimmunoprecipitation Assay (RIPA) buffer (P0013B, Beyotime, China) and centrifuged to collect the supernatant. Total protein was extracted and stored at –80 °C for subsequent Western blotting. For Western blotting, 500 µg of total protein from each sample was mixed with 5×SDS sample buffer at a 4:1 ratio and denatured by heating at 100 °C for 6 minutes. Sixty micrograms of denatured protein were loaded onto a 10% SDS-PAGE gel (PG212, Epizyme, Shanghai, China) and transferred to a polyvinylidene fluoride membrane (PVDF) membrane (10600023, Amersham, Germany). The membrane was blocked with a 5% skim milk solution for 1 hour, washed three times with Tris-Buffered Saline with Tween 20 (TBST) buffer (5 minutes each wash), and incubated overnight at 4 °C with primary antibodies against DDDDK-Tag (AE169, abclonal, China) and BMP-9 (abclonal, A10537, China) and GAPDH (abclonal, A19056, China) at a 1:1000 dilution. The DDDDK-Tag is an antibody specifically targeting the Flag tag. After three cycles of washing, the membrane was incubated with a secondary antibody (abclonal, AS014, China) at room temperature for 1 hour, followed by three additional washes with TBST. Signal detection was performed using an ECL enhanced chemiluminescence detection kit (34580, Thermo, Waltham, MA, USA). GAPDH expression was regarded as an endogenous control for normalization. Each sample's Western blotting experiment was repeated at least three times.

2.8 qPCR

Total RNA was extracted from BMSc and MG63 cells using TsingZol (TsingKe, Beijing, China) and quantified using agarose gel electrophoresis and Nanodrop oneC (Thermo, USA). Only RNA samples meeting quality criteria were used for subsequent analysis. First-strand cDNA was synthesized using the GoldenstarTM RT6 cDNA Synthesis Kit Ver.2 (TsingKe, Beijing, China). The qPCR experiments were conducted using the 2×T5 Fast qPCR Mix (SYBR Green I) (TsingKe, Beijing, China), with GAPDH mRNA serving as the endogenous reference gene for normalization. All procedures were performed according to the manufacturer's protocols. Relative gene expression levels were analyzed using the $2^{-\Delta\Delta Ct}$ method, with each result repeated at least three times. Specific primers are listed in Table 1.

Table 1. Primer sequences.

Primer Name	Sequences
BMP-9-F	CGCCGCAGTACATGATTGAC
BMP-9-R	GACCACGCTTCCTTTCAGGT
h-GAPDH-F	TCAAGGCTGAGAACGGGAAG
h-GAPDH-R	TCGCCCCACTTGATTTTGGA

2.9 Animal Modeling and Group Treatment

Twenty-four male New Zealand White rabbits, weighing between 2 kg to 2.2 kg, were provided by Byrness Weil biotech Ltd (Chongqin, China). The animal room maintained a 12-hour light/dark cycle, allowing free access to water and food for the experimental rabbits, with a temperature maintained between 23–25 °C. All experimental procedures and animal care were strictly conducted in accordance with the "Guide for the Care and Use of Laboratory Animals", and were approved by the Ethical Committee of Chongqing Medical Hospital (IACUC-CQMU-2023-0067). After one week of adaptive feeding, the animals entered the experiment.

A femoral condyle fracture model was constructed in 24 New Zealand White rabbits. Anesthesia was induced by administering 3% pentobarbital sodium (1 mL/kg) via ear vein injection. The animals were positioned supine and fixed. All surgical procedures were conducted under

strict aseptic conditions. A 5 cm longitudinal parapatellar incision was made, and the subcutaneous tissue, fascia, and muscles were dissected to expose the patella. After dislocation of the patella, the femoral condyle was exposed. An intercondylar femoral fracture was created using a saw. Following temporary reduction, a 2.5 mm diameter hole was drilled from the lateral side to the opposite cortex. Two different types of screws were used to fix the left and right legs of each rabbit. Specifically, the experimental group received multilayer Ad-BMP-9/BMSc/GT coated n-CDHA/PAA composite biomaterials screws. Two control groups were treated with medical metal screws and n-CDHA/PAA composite biomaterials screws, respectively.

Rabbits were sacrificed at 1, 4, 12, and 24 weeks post-surgery via intravenous air injection. Operated knee joints were harvested and stored in liquid nitrogen for subsequent analysis. Digital veterinary X-ray imaging systems (20111337C, Hangzhou Zhiyuan Medical Equipment Co., Ltd., Hangzhou, China) were used to take X-ray images of the surgical sites of the living rabbits at different time points (kVP: 58, mAs: 4.00, mA: 320). Micro-CT *in vivo* imaging system for small animals (IMAGING 100, Hefei Ruishi Medical Technology Co., Ltd., Hefei, China) was used to observe the material-bone interface integration at four time points and to measure the bone density adjacent to the interface. Scanning electron microscopy (SU8100, Hitachi, Japan) was used to observe the bone-screw interface of the rabbit knee joints in each group (3.0 kV $\times$ 1.0 k), and an energy-dispersive X-ray spectrometer attached to the scanning electron microscope was used to analyze the calcium deposition at the material-bone interface. Biomechanical testing was conducted to measure the interface binding strength between the material and bone tissue at four time points. The surface condition of the screws after push-out experiments at four time points was observed using scanning electron microscopy (SU8100, Hitachi, Tokyo, Japan).

2.10 Toluidine Blue Staining

The sample was fixed with 4% paraformaldehyde, decalcified with Ethylenediaminetetraacetic acid (EDTA) (DD0002, Leagene, Beijing, China), dehydrated with ethanol (64-17-5, Chuandong Chemical, Chongqing, China), transparent with xylene (1330-20-7, Chuandong Chemical, Chongqing, China), waxed in paraffin (80200-0007, Shitai, Hangzhou, China), then embedded, sliced and baked. The slices were dewaxed in xylene, dehydrated in ethanol, dipped in toluidine blue dye solution (G1032, Servicebio, Wuhan, China) for 5 min, washed, and differentiated into light blue background with 0.1% glacial acetic acid, and stopped by tap water washing. After dehydration and sealing, the slices were observed and recorded with Mshot MF53 microscope (Mingmei, Guangdong, China).

2.11 Masson Staining

The slices were processed by Masson trichromatic staining kit (Solarbio, Beijing, China) according to the instructions. The steps are as follows: Dip the prepared paraffin slices into mordant dye solution, let them act at room temperature for one night, and rinse them with running water. The sections were stained with lapis lazuli blue staining solution for 3 min, Mayer hematoxylin staining solution for 3 min, acidic ethanol differentiation solution until the tissues turned red completely, and washed with distilled water. The slices were dyed with ponceau magenta dye solution for 10 min, treated with phosphomolybdic acid solution for 10 min, and dyed with aniline blue dye solution for 5 min. After washing the slices with weak acid solution to remove aniline blue solution, continue to drip weak acid working solution to cover the slices for 2 min. The samples were dehydrated and sealed, then observed and recorded under a microscope (MF53, Mingmei, Guangzhou, China).

2.12 Verhoeff's van Gieson Staining

The sections were processed using the Eosin-Van Gieson (EVG) staining kit (Servicebio, Wuhan, China) according to the instructions, as follows: The paraffin sections were dyed with 5:2:2 mixed EVG A, B and C solutions for 5 min, and then dyed with EVG B dye solution diluted twice to control the differentiation until the elastic fibers were dark purple and the background was grayish white under the microscope. The EVG dyes D and E were mixed at a ratio of 1:9, and the slices were dyed for 12 min and washed with water. Finally, the slices were dehydrated and sealed, and observed and recorded under a microscope (MF53, Mingmei, China).

2.13 Statistical Analysis

Experimental data were presented as mean $\pm$ standard error, and comparisons between groups were performed using the T-test, and GraphPad Prism 8 software (GraphPad Software, Inc., San Diego, CA, USA) was used for data analysis and visualization. Differences were considered statistically significant at $p < 0.05$.

3. Results

3.1 GT-Loaded Ad-BMP-9/BMSc Promotes the Proliferation and Differentiation of MG63 Cells

Firstly, we successfully established BMP-9 overexpressing BMSc cells by transfecting the Flag-tagged BMP-9 recombinant adenovirus. Successful transfection of BMSc cells was confirmed by a significant increase in both *BMP-9* gene and DDDDK-Tag protein expression levels, as depicted in Fig. 1A,B ($p < 0.05$). Subsequently, we constructed Ad-BMP-9/BMSc/GT by loading Ad-BMP-9/BMSc onto GT. Ad-BMP-9/BMSc/GT was co-cultured with MG63 cells for 10 days, and the cell proliferation and differentiation capabilities were assessed on days 1, 5, and 10, respectively. Ad-BMP-9/BMSc/GT significantly en-

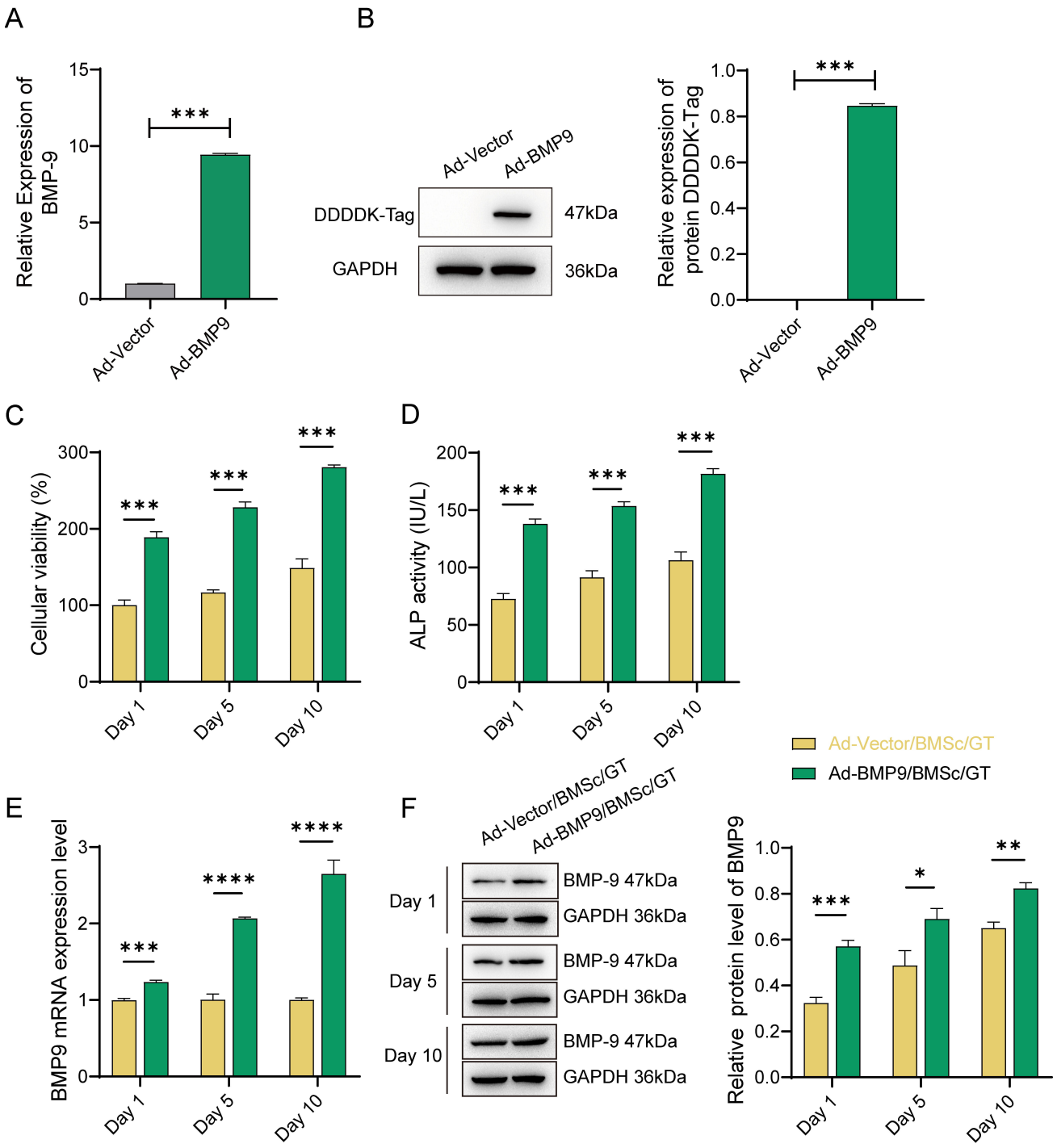

Fig. 1. The Effect of Gelatin (GT)-Loaded Adenovirus (Ad)-Bone Morphogenetic Protein 9(BMP-9)/Bone Marrow Mesenchymal Stem Cells (BMSc) on the Proliferation and Differentiation of MG63 Cells. (A) Expression of the *BMP-9* gene and (B) DDDDK-Tag protein after transfection of BMSc cells with recombinant adenovirus (Ad-BMP-9) for 48 hours. (C) Cell viability assays performed on days 1, 5, and 10 during the 10-day co-culture of Ad-BMP-9/BMSc/GT with MG63 cells. (D) alkaline phosphatase (ALP) activity assay. (E) Detection of *BMP-9* gene levels in cells on days 1, 5, and 10. (F) Relative expression of BMP-9 protein in cells on days 1, 5, and 10. *, Indicates a statistically significant difference between the two groups with p-value < 0.05; **, p-value < 0.01; ***, p-value < 0.001; ****, p-value < 0.0001. n = 3.

hanced both MG63 cell proliferation and ALP activity compared to the Ad-vector/BMSc/GT group (Fig. 1C,D, $p < 0.05$), suggesting that Ad-BMP-9/BMSc/GT promotes both proliferation and differentiation of MG63 cells. Furthermore, we monitored the changes in *BMP-9* gene and protein expression levels in MG63 cells. The results showed

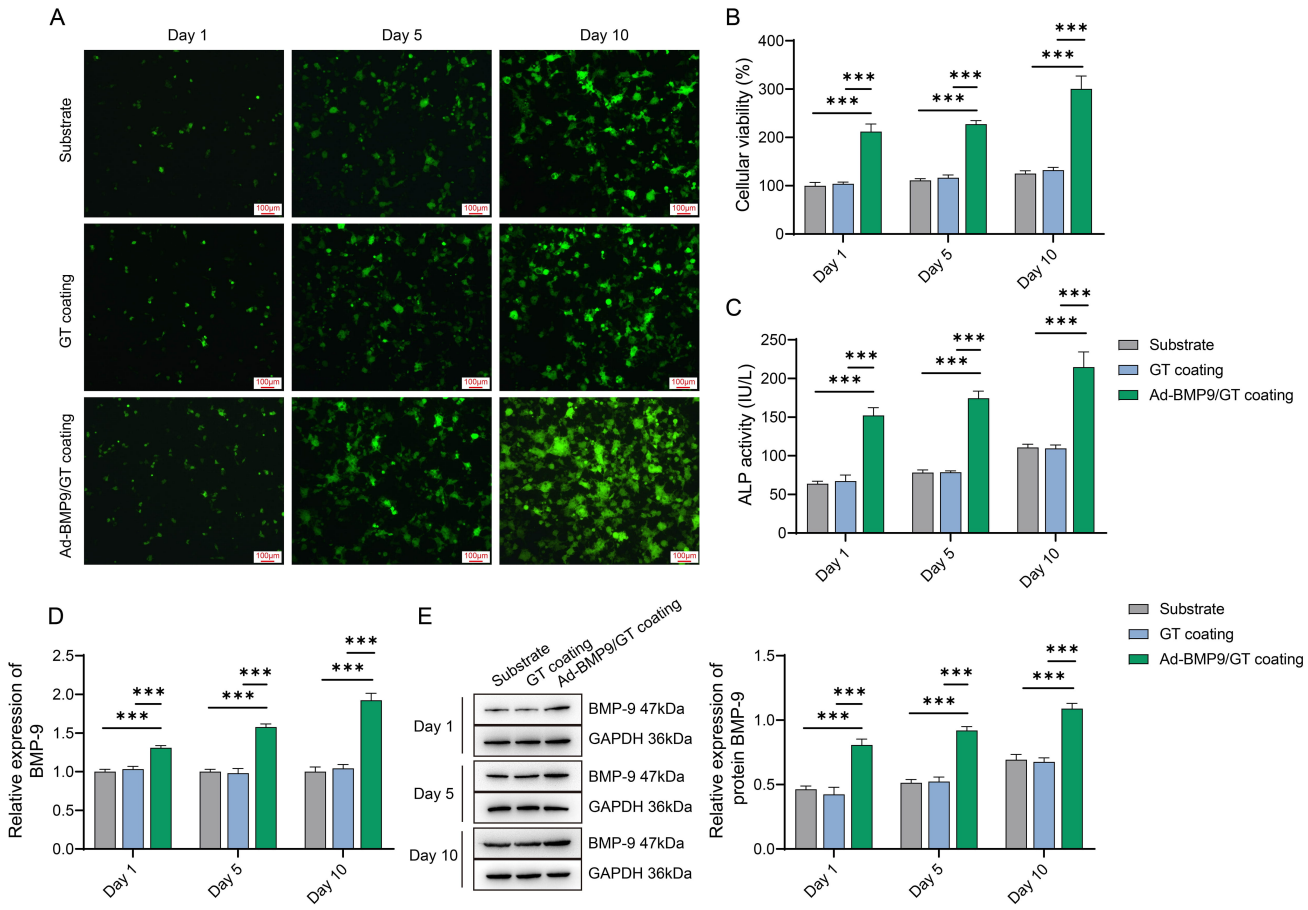

Fig. 2. Assessment of Biocompatibility of Multilayer Ad-BMP-9/BMSc/GT Coated nano-calcium deficient hydroxyapatite/polyamino acid(n-CDHA/PAA) Composite Biomaterials with MG63 Cells. (A) Microscopic observation of MG63 cell growth on the material surface at three time points. Scale bars: 100 µm. (B) Cell Counting Kit-8 (CCK-8) assay for the proliferation of MG63 cells at three time points. (C) ALP activity assay for the viability of MG63 cells at three time points. (D) Quantitative Polymerase Chain Reaction (q-PCR) detection of BMP-9 mRNA expression in MG63 cells at three time points. (E) Western blot (WB) detection of BMP-9 protein expression in MG63 cells at three time points. ***, Indicates a statistically significant difference between groups with p-value $<$ 0.001. n = 3.

that the BMP-9 mRNA and protein expression levels in MG63 cells of the Ad-BMP-9/BMSc/GT group gradually increased over time (Fig. 1E,F, $p < 0.05$), which is consistent with the promotion of MG63 cell proliferation and differentiation.

3.2 Multilayer Ad-BMP-9/BMSc/GT Coating on n-CDHA/PAA Composite Biomaterials Exhibits Good Biocompatibility with MG63 Cells

To evaluate the *in vitro* biocompatibility of the multilayer Ad-BMP-9/BMSc/GT coated n-CDHA/PAA composite biomaterials, we conducted cell cultures on the experimental group with the multilayer Ad-BMP-9/BMSc/GT coating on n-CDHA/PAA composite biomaterials (Ad-BMP-9/GT coating), the control group with a single layer of GT coating on n-CDHA/PAA composite biomaterials (GT coating), and the n-CDHA/PAA control group (Substrate), with a series of assessments performed on days 1, 5, and 10. To visually observe the growth of cells on the material surface, we conducted microscopic observations. The results showed that on the first day, there was not much cell growth in all groups. In the Ad-BMP-9/GT coating group, MG63 cells exhibited good spreading and growth morphology on the material surface, with a significant increase in cell numbers (Fig. 2A). Concurrently, CCK-8 assay results indicated that the proliferation capacity of MG63 cells in the Ad-BMP-9/GT coating group was significantly enhanced compared to the Substrate group, and this capacity continued to improve over time (Fig. 2B, $p < 0.05$). Furthermore, ALP activity assay results showed that the ALP activity of MG63 cells in the Ad-BMP-9/GT coating group was markedly higher than that of the control group, indicating that the Ad-BMP-9/GT coating can promote the differentiation of MG63 cells (Fig. 2C, $p < 0.05$). Lastly, we detected the mRNA and protein expression levels of BMP-9 in MG63 cells. The results showed that compared to the Substrate group, the mRNA and protein expression levels of

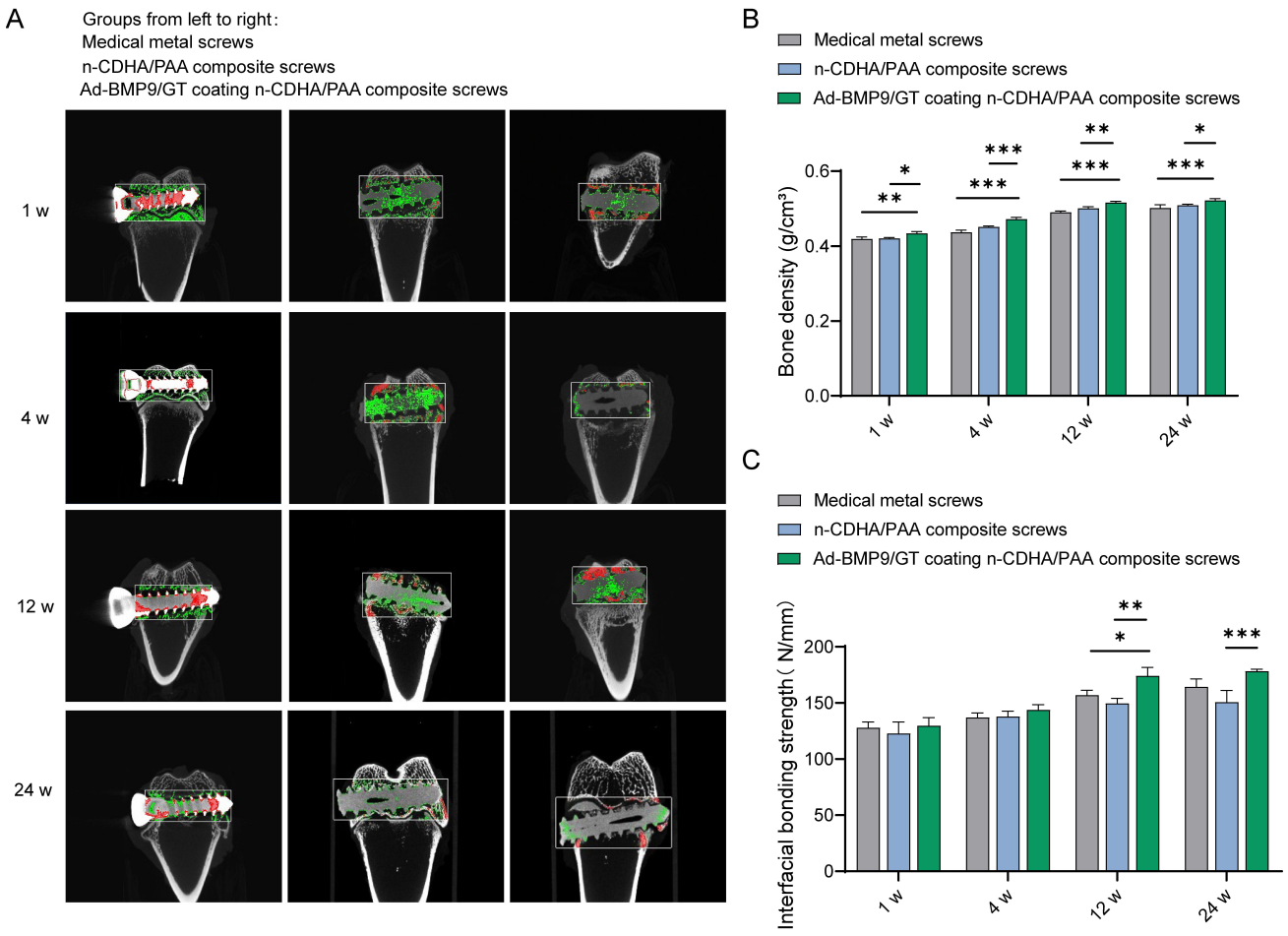

Fig. 3. Assessment of the Integration of Multilayer Ad-BMP-9/BMSc/GT Coated n-CDHA/PAA Composite Biomaterials with Neo-tissue at Rabbit Bone Wounds. (A) Micro-CT imaging to observe the integration at the composite biomaterial-bone interface at four time points (1 week, 4 weeks, 12 weeks, 24 weeks), red represents cortical bone, and green represents trabecular bone. (B) Measurement of bone density adjacent to the composite biomaterial-bone interface. (C) Biomechanical testing to detect the interface binding strength between the composite biomaterials and bone tissue at 1 week, 4 weeks, 12 weeks, and 24 weeks. *, Indicates a statistically significant difference between groups with p-value < 0.05; **, p-value < 0.01; ***, p-value < 0.001. n = 3.

BMP-9 in MG63 cells in the Ad-BMP-9/GT coating group were significantly elevated (Fig. 2D,E, $p < 0.05$), and these expression levels gradually increased over time. This suggests that the Ad-BMP-9/GT coating can promote the proliferation and differentiation of MG63 cells by continuously releasing BMP-9.

3.3 Multilayer Ad-BMP-9/BMSc/GT Coating Enhances the Integration of Neo-tissue at the Bone Wound and Screw Surface

In vitro experimental results indicate that the multilayer Ad-BMP-9/BMSc/GT coated n-CDHA/PAA composite biomaterials exhibit good biocompatibility with MG63 cells and effectively promote the attachment, proliferation, differentiation, and expression of BMP-9 in these cells. Subsequently, we constructed an intercondylar femoral fracture model in rabbits and fixed it with Ad-BMP9/GT coated n-CDHA/PAA composite screws, medical metal screws, and n-CDHA/PAA composite screws, followed by a series of assessments at 1, 4, 12, and 24 weeks postoperatively. Micro-CT images revealed that at one week post-surgery, there were clear fracture gaps visible in the knee joint samples of all groups; at four weeks post-surgery, the fracture gaps were less distinct compared to the first week, indicating that new bone formation occurs over time; at twelve weeks post-surgery, the fracture gaps had essentially healed, with no obvious signs of fracture visible in the Micro-CT images, and no abnormalities in the overall samples; the bone density of the knee joint samples in all groups gradually increased over time, with the Ad-BMP9/GT coated n-CDHA/PAA composite screws showing the best results at later stages (Fig. 3A,B, $p < 0.05$). Biomechanical testing results showed that medical metal screws had certain advantages in terms of maximum load during early bone fixation; as the duration of screw fixation extended, the fixation strength of the composite

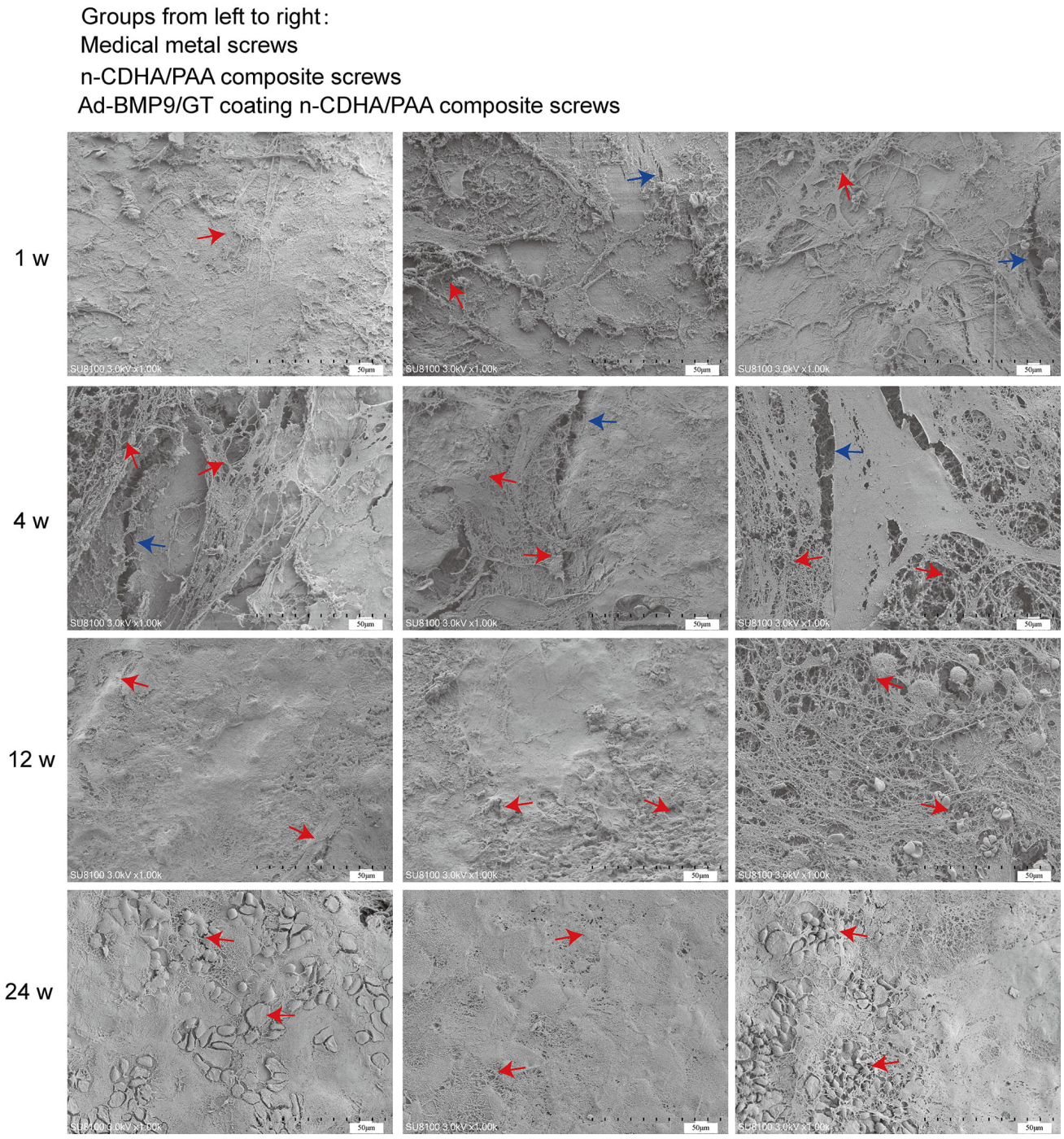

Fig. 4. Scanning electron microscopy (SEM) to observe the interface between the composite biomaterials and bone tissue at 1 week, 4 weeks, 12 weeks, and 24 weeks. Red arrow: three-dimensional structure; Blue arrow: crack. Scale bars: 50 µm.

biomaterials screws coated with the multilayer Ad-BMP-9/BMSc/GT coating was higher than other two groups, indicating that Ad-BMP9/GT coated n-CDHA/PAA composite screws have good osseointegration capabilities, which help to enhance the integration of neo-tissue at the bone wound and the screw surface (Fig. 3C, $p < 0.05$). SEM observations showed that at one week post-surgery, there was a small amount of neo-tissue at the bone interface in all groups; at four weeks post-surgery, the amount of neo-tissue at the bone interface increased in all groups, but cracks were observed; at twelve weeks post-surgery, there was more neo-tissue at the bone interface, which was more tightly packed, especially in the Ad-BMP9/GT coated n-CDHA/PAA composite screws group where a clear three-dimensional reticular structure was visible, indicating that the multilayer Ad-BMP-9/BMSc/GT coating on the composite biomaterials screws aids in the recovery after bone trauma; the SEM results at twenty-four weeks post-surgery

showed that the bone interfaces in all groups had recovered well, indicating that the materials implanted long-term in animals had no side effects (Fig. 4).

3.4 Multilayer Ad-BMP-9/BMSc/GT Coated n-CDHA/PAA Composite Biomaterials Can Promote Neo-tissue Formation at Rabbit Bone Wounds

X-ray images of the surgical sites of the rabbit femur show that none of the screws in any group exhibited loosening or detachment (Fig. 5A). Starting from the 4th week, obvious neo-tissue attachment was observed on the surface of the screws in all groups. By the 12th week, the neo-tissue was more tightly integrated with the screw surfaces, with the Ad-BMP9/GT coated n-CDHA/PAA composite screws showing the most abundant new bone tissue, visible cells closely adhering to the material surface. By the 24th week, the surfaces of the screws in all groups were covered with biological tissue, indicating that over time, there was no rejection phenomenon between the biological body and the materials (Fig. 5B). Calcium deposition was significantly enhanced at the material-bone interface in Ad-BMP9/GT coated n-CDHA/PAA composite screws compared to medical metal screws at both 12 w and 24 w (Fig. 5C, $p < 0.05$). Further supporting the ability of multilayer Ad-BMP-9/BMSc/GT coated n-CDHA/PAA composite biomaterials to promote bone tissue regeneration.

3.5 Multilayer Ad-BMP-9/BMSc/GT Coated n-CDHA/PAA Composite Biomaterials Can Promote Growth of collagen fibers at Rabbit Bone Wounds

To determine the effect of Ad-BMP-9/BMSc/GT Coated n-CDHA/PAA Composite Biomaterials on chondroitin sulfate and collagen fiber growth in bone tissue, we observed rabbit bone wounds by multiple staining.

Based on the metachromatic property of chondroitin sulfate, which stains purple-red with toluidine blue, we conducted measurements of the staining results, including the area, depth of the stained regions, and their proportions in the total area. Statistical analysis revealed no significant differences in chondroitin sulfate content among the groups at weeks 1 and 4. However, at week 12, the chondroitin sulfate content in the bone tissue of the Ad-BMP-9/BMSc/GT coated n-CDHA/PAA group was significantly higher than that in the n-CDHA/PAA group ($p < 0.05$). Furthermore, at both weeks 24, the chondroitin sulfate content in the Ad-BMP-9/BMSc/GT coated n-CDHA/PAA group was significantly higher than that in the Medical metal screw group (Fig. 6, $p < 0.05$).

The results of Massonstaining and Verhoeff's vangiesonstaining showed that there was no significant difference in the growth of collagen fibers in the bone tissue of each group at the 1th and 4th weeks, but at the 12th and 24th weeks, Ad-BMP-9/GT Coated n-CDHA/PAA composite screws group exhibited the most abundant growth of collagen fibers in the bone tissue (Fig. 7, $p < 0.05$).

4. Discussion

Bone tissue engineering has emerged as a promising field for addressing bone defects and promoting bone regeneration. The ideal osseointegration requires that bone tissue can be directly deposited onto the implant surface, form some kind of chemical bond with the bone tissue, and also promote rapid cell differentiation and growth (Osteoinduction) [17]. Current methods typically involve the use of biomaterials, growth factors, and stem cells [18]. In recent years, the field of bone tissue engineering has made progress in the design of biomaterials and cell therapies. Nanomaterials, due to their large surface area, are conducive to the adhesion of cells, proteins, etc., and have good mechanical properties and excellent biocompatibility, which have been widely used in bone tissue engineering [19]. At present, the nanocrystalline structure of hydroxyapatite, which is close to the crystal structure and size of human bone tissue, is well synthesized and studied, capable of forming a strong osteogenic bond with bone tissue [20]. We have previously developed n-CDHA/PAA composite biomaterials, which have been confirmed to have good biocompatibility and biomechanics both *in vitro* and *in vivo* [21,22]. However, to promote faster bone healing and rapid differentiation and growth, it is still necessary to improve the biocompatibility, osteoconductive properties, and osteogenic potential of these materials.

The incorporation of growth factors (GF) such as BMPs, Fibroblast Growth Factors (FGFs), Insulin-like Growth Factors I/II (IGF I/II), and Transforming Growth Factor-β (TGF-β), into bioactive coatings has been shown to enhance osteoprogenitor and osteoblast cell proliferation and differentiation, stimulate collagen matrix and apatite phase synthesis, and extend the lifespan of bone implants [23,24]. The application of bone growth factors in bone regeneration is widely recognized, with BMPs being the primary focus. Studies utilizing heterotopic bone formation models have compared the effects of 14 different BMPs on bone regeneration and found that BMP-2, 6, 7, and 9 can effectively induce bone formation using adenovirus BMP-transduced C2C12 cell lines [25]. The application of bone growth factors in bone regeneration is widely recognized, with BMPs being the primary focus. Studies utilizing heterotopic bone formation models have compared the effects of 14 different BMPs and revealed that BMP-2, 6, 7, and 9 effectively induce bone formation when delivered via adenovirus BMP-transduced C2C12 cell lines [26]. Therefore, there are still challenges in controlling the sustained release of growth factors and promoting effective integration of biomaterials with surrounding bone tissue. Our study addresses this deficiency by combining n-CDHA/PAA composite biomaterials with overexpression of BMP-9 using Ad-BMP-9/BMSc/GT coatings. This study explores the potential of this material in promoting bone regeneration. Our results indicate that this new approach not only promotes the proliferation and differentiation of osteoblasts *in*

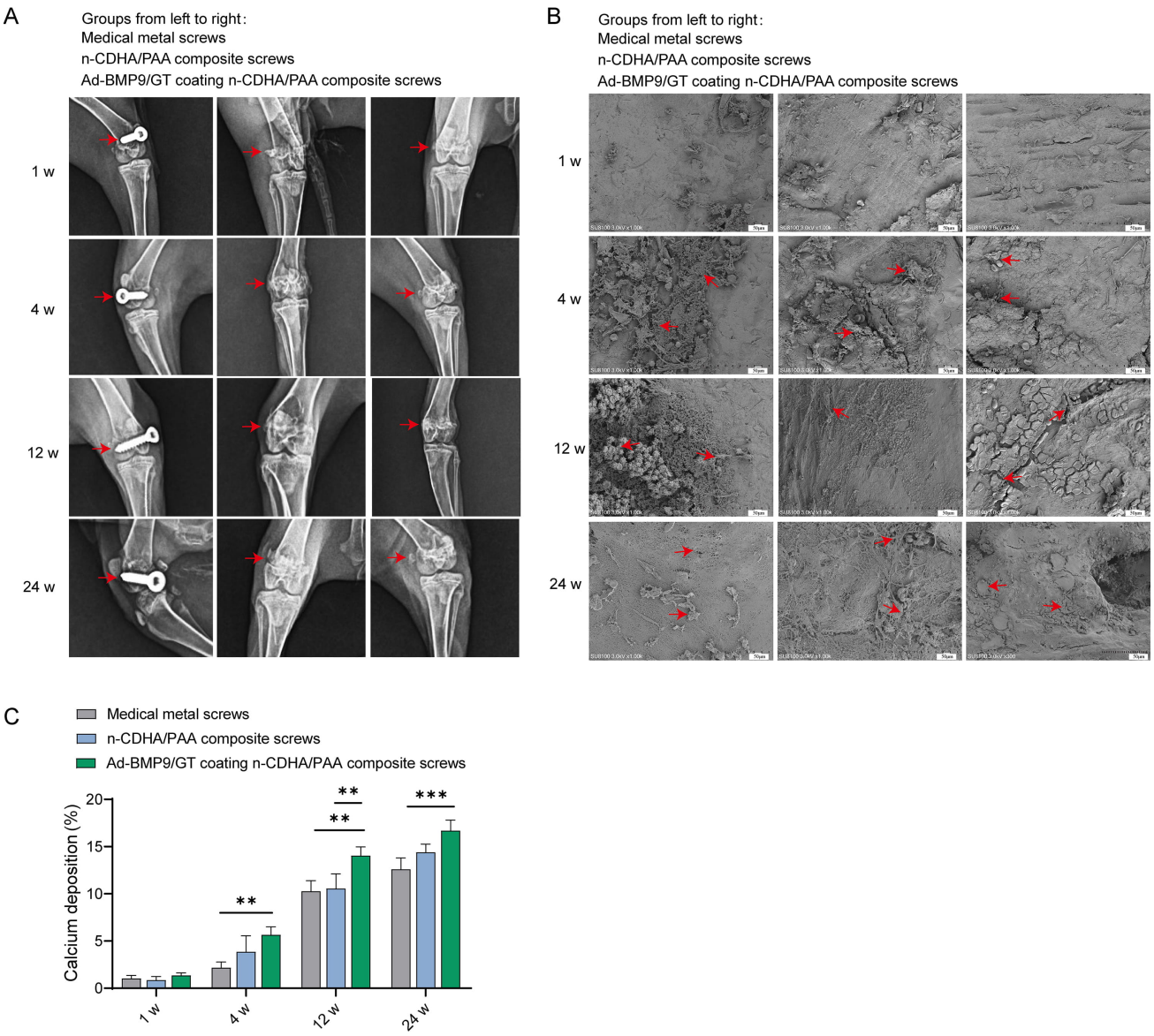

Fig. 5. The Impact of Multilayer Ad-BMP-9/BMSc/GT Coated n-CDHA/PAA Composite Biomaterials on Neo-tissue Formation at Rabbit Bone Wounds. (A) X-ray imaging (anteroposterior view) of screw loosening at the surgical sites of each group at 1 week, 4 weeks, 12 weeks, and 24 weeks post-surgery. (B) Scanning electron microscopy (SEM) observation of the screw surface conditions after push-out experiments at 1 week, 4 weeks, 12 weeks, and 24 weeks. Scale bars: 50 µm. (C) X-ray energy dispersive spectroscopy (EDS) analysis of calcium deposition at the material-bone interface at 1 week, 4 weeks, 12 weeks, and 24 weeks. **, Indicates a statistically significant difference between groups with p-value < 0.01; ***, p-value < 0.001. n = 3. Red arrow: three-dimensional structure.

vitro but also significantly improves *in vivo* bone healing and biomechanical integration, showing promise as a potential strategy for bone repair and regeneration.

Stem cells have shown great potential in repairing bone defects, with Bone Marrow Stromal Cells (BMSCs) being an ideal source for bone defect repair due to their ease of accessibility, strong self-renewal capacity, and prominent osteogenic differentiation ability [27]. Additionally, studies have confirmed the ability of BMSCs to effectively repair bone defects in animal models [28]. In this study, we first successfully constructed BMSCs with overexpression of the *BMP-9* gene. Compared to the GT group, GT-supported Ad-BMP-9/BMSCs could effectively promote the proliferation and differentiation of MG63 cells by continuous release of BMP-9. Therefore, we speculate that constructing BMSCs with overexpression of the *BMP-9* gene and combining them with GT delivery could effectively promote the repair of bone defects. BMPs belong to the Transforming Growth Factor-β superfamily and were first discovered by Marshall Urist [29]. BMP-9 is a member of the BMP family, similar to the well-studied BMP-2, BMP-4, and BMP-7, and possesses the ability to me-

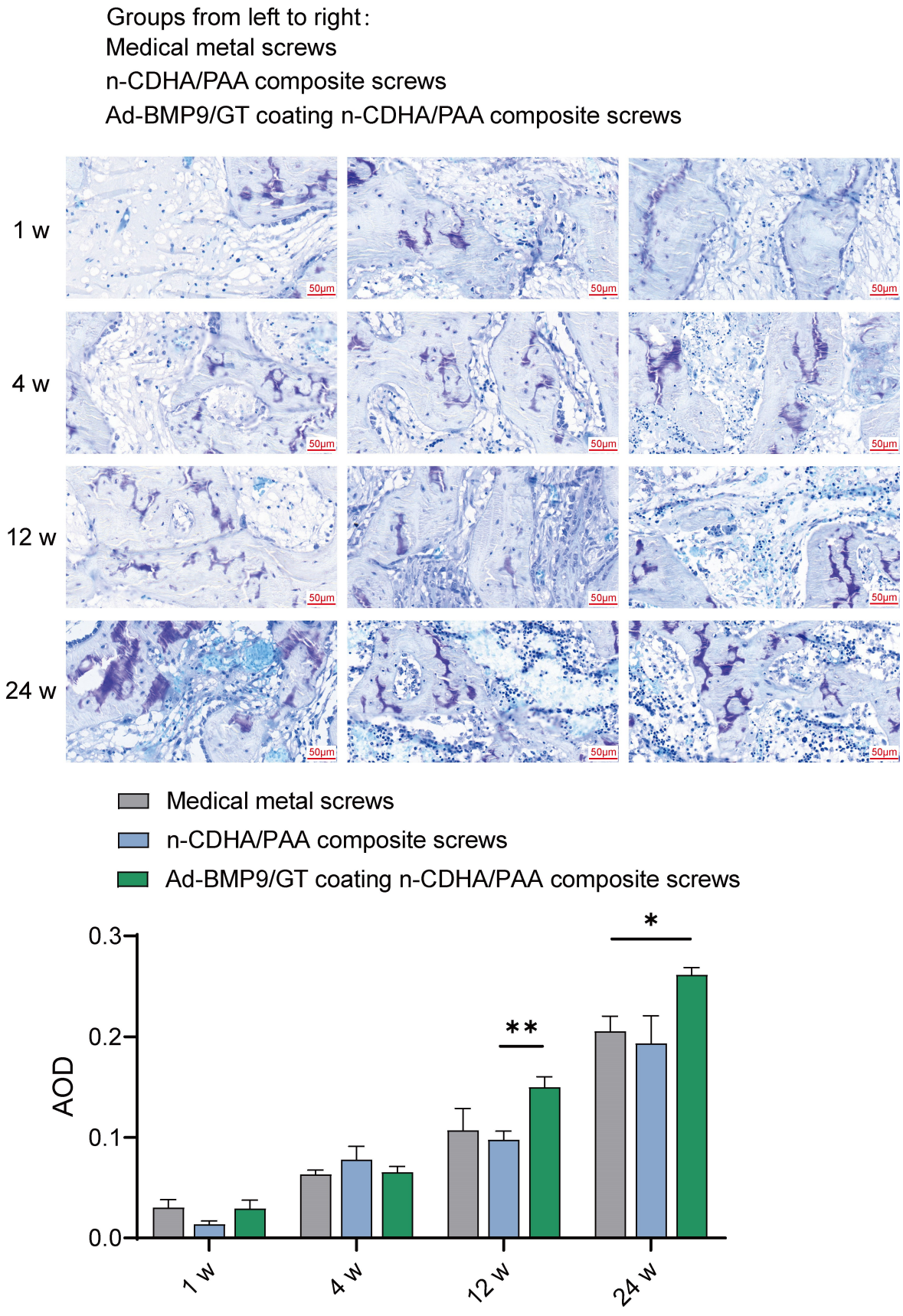

Fig. 6. The Impact of Multilayer Ad-BMP-9/BMSc/GT Coated n-CDHA/PAA Composite Biomaterials on Chondroitin Sulfate at Rabbit Bone Wounds by Toluidine Blue Staining. *, Indicates a statistically significant difference between groups with p-value $<$ 0.05; **, p-value $<$ 0.01. n = 3. Scale bars: 50 μm.

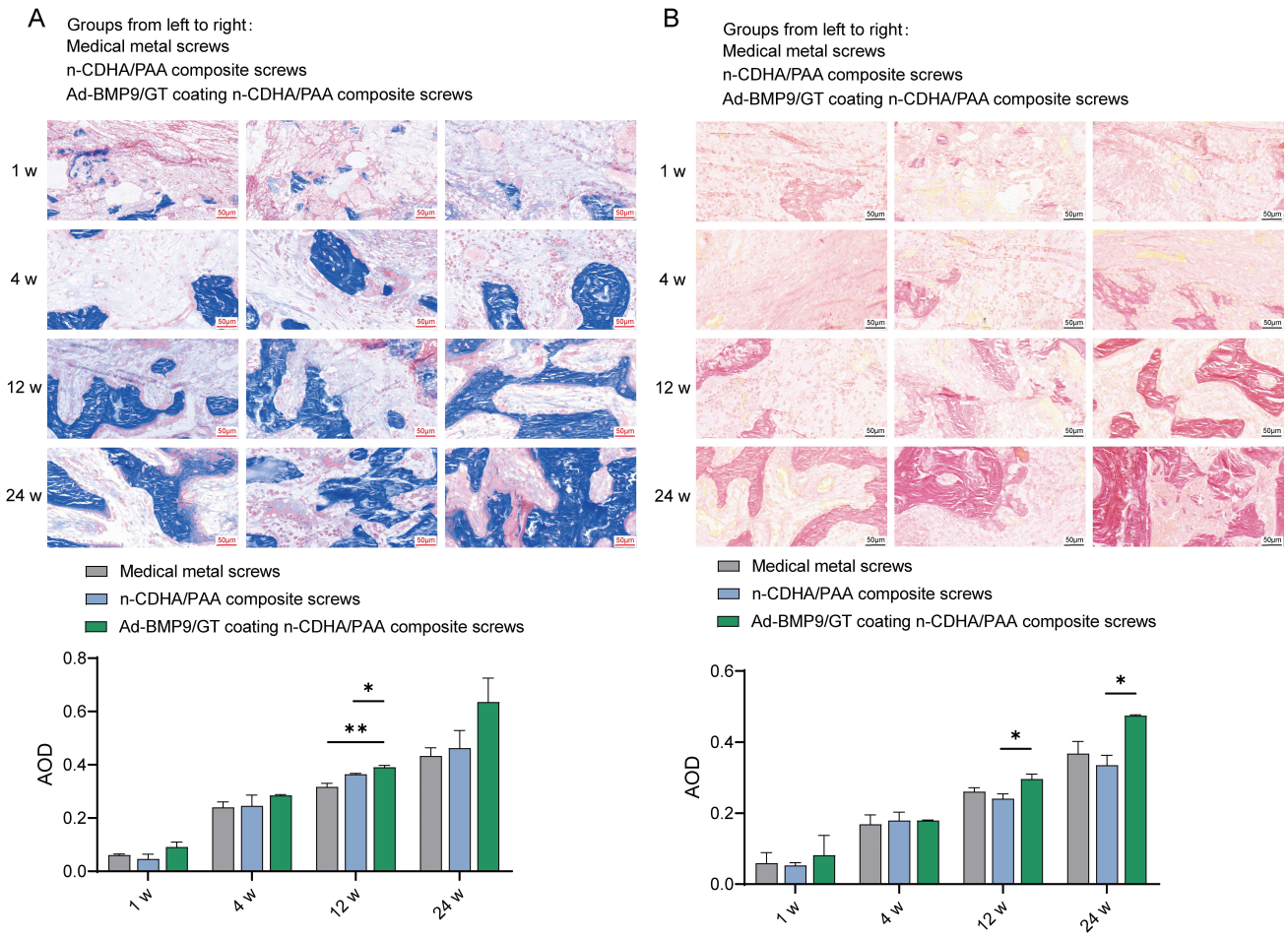

Fig. 7. The Impact of Multilayer Ad-BMP-9/BMSc/GT Coated n-CDHA/PAA Composite Biomaterials on Collagen Fiber Growth at Rabbit Bone Wounds. (A) Masson staining. (B) Verhoeff's van gieson staining. *, Indicates a statistically significant difference between groups with p-value < 0.05; **, p-value < 0.01. n = 3. Scale bars: 50 µm.

diate the osteogenic differentiation of Mesenchymal Stem Cells (MSCs). Compared to clinically used recombinant human BMP-2 (rhBMP-2) and rhBMP-7, BMP-9 has been proven to more effectively promote the activity of human osteoblasts [30] and the osteogenic differentiation of mouse mesenchymal stem cells [31]. To overcome the uncontrollable release rate of BMPs in bone repair and issues such as excessive bone growth, researchers have made some progress in finding better carriers for BMPs to control their release and bone repair functions. *In vivo* studies by Wang *et al.* [32] revealed that poly-lactic acid glycolic acid (PLGA) scaffolds loaded with BMP-9 + P-15 peptide hydrogel promoted increased expression of ALP, RUNX2 (Runt-related transcription factor 2), and OCN (Osteocalcin) in MSCs compared to controls. This suggests that BMP-9 can better promote the osteogenic differentiation of MSCs. At the same time, the study also observed more new bone formation in the BMP-9 + P-15 peptide hydrogel + PLGA group in a rabbit bone defect model. Shi *et al.* [33] reported that the combined application of Bioactive Glass (Bioglass) + BMP-9 could better promote osteogenic differentiation. It was observed that *in vivo*, compared to the use of Bio-glass alone, the BMP-9 + Bioglass group had higher ALP activity, and the expression levels of RUNX2 and OSX were also significantly upregulated in the presence of BMP-9. However, the carriers used for BMP-9 in these studies still have certain limitations in terms of biocompatibility and degradation rate.

Our study presents a novel method for the sustained delivery of BMP-9 and enhanced bone-biomaterial integration through a multi-layer coating system. We developed a composite biomaterial with multi-layer Ad-BMP-9/BMSc/GT coatings on n-CDHA/PAA and found it to provide an excellent environment for cell adhesion. Over time, the proliferation capacity of MG63 cells and the expression levels of BMP-9 in the Ad-BMP-9/GT coating group continuously improved, indicating that this coating can promote cell differentiation, endowing them with greater osteogenic potential, similar to the results of Wang *et al.* [32] and Shi *et al.* [33]. Our method utilizes a multilayer GT-based system combined with BMP-9 expressing BMSc cells, offering several advantages. GT is a natu-

ral biomaterial, and its use helps to enhance biocompatibility and reduce the risk of inflammatory responses [34]. The multi-layer coating system allows for controlled and sustained release of BMP-9, thereby promoting bone formation. Additionally, incorporating BMSc cells overexpressing BMP-9 in the coating facilitates the integration of cells with the biomaterial, promoting bone regeneration and bone-biomaterial integration. These results offer a potential strategy for bone tissue engineering, with the expectation of enhancing the bioactivity of bone repair materials.

Internal fixation screws are commonly used to stabilize strong metaphyseal fractures, particularly in the femoral or humeral shaft [35]. Our previous research demonstrated the excellent biocompatibility and biodegradability of n-CDHA/PAA composite material when fabricated into internal fixation screws for an articular fracture animal model [22]. This study evaluated the bone repair effects of multilayer Ad-BMP-9/BMSc/GT coated n-CDHA/PAA composite biomaterials (experimental group) compared to conventional metal screws and n-CDHA/PAA composite screws (control group) by constructing an intercondylar femoral fracture model in rabbits. Micro-CT images showed that the Ad-BMP9/GT coated n-CDHA/PAA composite screws group exhibited faster fracture gap healing and higher bone density, demonstrating excellent osseointegration capabilities. Biomechanical testing results indicated that Ad-BMP9/GT coated n-CDHA/PAA composite screws showed advantages in fixation strength, especially after long-term fixation, where their fixation strength was significantly higher than that of traditional medical metal screws. This suggests that the presence of multilayer coatings enhances the binding ability of the screws with the surrounding bone tissue. More importantly, the Ad-BMP9/GT coated n-CDHA/PAA composite screws group formed dense neo-tissue at the bone interface 12 weeks post-surgery, presenting a clear three-dimensional reticular structure. This indicates that the multilayer coatings on the composite biomaterial screws contribute to the promotion of bone wound repair and recovery. The potential application of this technology lies in improving the success rate of fracture repair, reducing postoperative complications, and possibly shortening recovery time, which is of significant importance to the clinical practice of orthopedic surgery.

Traditional bone repair materials often struggle to form a strong bond with bone tissue, leading to suboptimal repair outcomes [36]. Regeneration of bone tissue is a critical step in the promotion of bone repair by implants; it enhances the fixation and stability of the implant, improves biocompatibility, promotes the long-term functionality of the implant, and reduces the risk of infection [37]. Our results indicate that from 4 weeks post-surgery, noticeable neo-tissue attachment was observed on the surfaces of screws in all groups, and chondroitin sulfate and collagen fibers appeared to increase. By the 12th week, the neo-tissue was more tightly integrated with the screw surfaces, particularly in the Ad-BMP9/GT coated n-CDHA/PAA composite biomaterial screws group, where the new bone tissue was the most abundant and closely adhered to the material surface, and chondroitin sulfate and collagen fibers showed significant growth. By the 24th week, the surfaces of the screws in all groups were covered with biological tissue, indicating no rejection phenomena between the material and the biological entity, demonstrating excellent biocompatibility. Moreover, the multi-layer coating helps to promote the calcification process, thereby enhancing the regenerative and reparative capacity of bone tissue. X-ray imaging showed that no screws in any group exhibited loosening or detachment at various time points post-surgery, indicating that the fixation performance of the screws in all tested groups was satisfactory and met clinical requirements.

The multi-layer Ad-BMP-9/BMSc/GT coated n-CDHA/PAA composite biomaterials developed in this study can sustain the release of BMP-9, promote bone tissue regeneration, and effectively enhance the integration of neo-tissue at the bone wound with the material surface, significantly improving the bioactivity of bone repair materials. Compared to traditional bone repair materials, this approach exhibits greater osseointegration capacity and better bone repair outcomes. These findings are of significant clinical application value and have promising prospects for the development of new orthopedic repair materials, especially in the repair of complex fractures and the treatment of bone defects. While our research results are encouraging, it is also necessary to acknowledge certain limitations: the study followed up with animals for 24 weeks, which is relatively short for assessing the long-term biocompatibility and degradation of the multi-layer coating system. Further long-term studies are required to investigate the long-term effects of this method. Further investigation of the biodegradation products and their potential impact on surrounding tissues is essential to ensure long-term safety and efficacy. Additionally, exploring the optimal number of layers, thickness, and composition of the coating can further enhance the efficacy of this system. To successfully apply this multi-layer coating system to clinical practice, comprehensive pre-clinical studies are needed, including large animal models and assessments of safety and efficacy in clinical settings.

5. Conclusion

This study, based on multilayer Ad-BMP-9/BMSc/GT coated n-CDHA/PAA composite biomaterials, systematically assessed their potential in promoting bone tissue regeneration. Through *in vitro* and *in vivo* experiments, we verified the significant effects of this novel biomaterial in enhancing MG63 cell adhesion, promoting MG63 cell proliferation and differentiation, and accelerating fracture healing. Notably, the Ad-BMP-9/BMSc/GT coated n-CDHA/PAA composite biomaterial screws demonstrated

excellent osseointegration capabilities and biomechanical performance in a rabbit intercondylar femoral fracture model. These results indicate that the multilayer coating system not only effectively releases the growth factor BMP-9 to promote bone formation but also improves the integration of the biomaterial with surrounding bone tissue, thereby enhancing the bioactivity of bone repair materials and their potential for clinical application. This study provides strong scientific evidence for the development of innovative bone repair materials and lays a solid foundation for their clinical application. Future work will continue to explore the broad application and promotion of this multilayer coating system in the repair of complex fractures and the treatment of bone defects.

Availability of Data and Materials

The datasets generated during the current study will be available form the corresponding author upon a reasonable request.

Author Contributions

QY and YL: substantial contributions to the conception or design of the work, and drafted the manuscript; RW, LD and AH: the acquisition and analysis of data for the work; DZ and ZD: interpretation of data for the work, and reviewing the manuscript. All authors contributed to and approved the final manuscript. All authors contributed to editorial changes in the manuscript. All authors have participated sufficiently in the work and agreed to be accountable for all aspects of the work.

Ethics Approval and Consent to Participate

All animal experiments were performed in accordance with the guidelines of the Chongqing Medical Hospital Animal Care and Use Committee (IACUC) and were approved by the Ethical Committee of Chongqing Medical Hospital (IACUC-CQMU-2023-0067).

Acknowledgment

We would like to acknowledge the hard and dedicated work of all the staff that implemented the intervention and evaluation components of the study.

Funding

This study was supported by the General Project of Chongqing Municipal Natural Science Foundation (cstc2021jcyj-msxmX0832) and the Doctor Through Train Project of Chongqing Science and Technology Commission (CSTB2022BSXM-JCX0072).

Conflict of Interest

The authors declare no conflict of interest.

References

[1] Balasundaram G, Storey DM, Webster TJ. Molecular plasma deposition: biologically inspired nanohydroxyapatite coatings on anodized nanotubular titanium for improving osteoblast density. International Journal of Nanomedicine. 2015; 10: 527–535.

[2] Liu Y, Rath B, Tingart M, Eschweiler J. Role of implants surface modification in osseointegration: A systematic review. Journal of Biomedical Materials Research. Part a. 2020; 108: 470–484.

[3] Witzdam L, Garay-Sarmiento M, Gagliardi M, Meurer YL, Rutsch Y, Englert J, *et al*. Brush-Like Coatings Provide a Cloak of Invisibility to Titanium Implants. Macromolecular Bioscience. 2024; 24: e2300434.

[4] Ching HA, Choudhury D, Nine MJ, Abu Osman NA. Effects of surface coating on reducing friction and wear of orthopaedic implants. Science and Technology of Advanced Materials. 2014; 15: 014402.

[5] Liu C, Yu K, Bai J, Tian D, Liu G. Experimental study of tendon sheath repair via decellularized amnion to prevent tendon adhesion. PloS One. 2018; 13: e0205811.

[6] Yan T, Zhang H, Huang D, Feng S, Fujita M, Gao XD. Chitosan-Functionalized Graphene Oxide as a Potential Immunoadjuvant. Nanomaterials (Basel, Switzerland). 2017; 7: 59.

[7] Grzeskowiak RM, Schumacher J, Dhar MS, Harper DP, Mulon PY, Anderson DE. Bone and Cartilage Interfaces With Orthopedic Implants: A Literature Review. Frontiers in Surgery. 2020; 7: 601244.

[8] Lu H, Wu PF, Ma DL, Zhang W, Sun M. Growth Factors and Their Roles in Multiple Sclerosis Risk. Frontiers in Immunology. 2021; 12: 768682.

[9] Wang R, Liu W, Du M, Yang C, Li X, Yang P. The differential effect of basic fibroblast growth factor and stromal cell derived factor 1 pretreatment on bone morrow mesenchymal stem cells osteogenic differentiation potency. Molecular Medicine Reports. 2018; 17: 3715–3721.

[10] Wang JJ, Liu YL, Sun YC, Ge W, Wang YY, Dyce PW, *et al*. Basic Fibroblast Growth Factor Stimulates the Proliferation of Bone Marrow Mesenchymal Stem Cells in Giant Panda (Ailuropoda melanoleuca). PloS One. 2015; 10: e0137712.

[11] Li R, Yan Z, Ye J, Huang H, Wang Z, Wei Q, *et al*. The Prodomain-Containing BMP9 Produced from a Stable Line Effectively Regulates the Differentiation of Mesenchymal Stem Cells. International Journal of Medical Sciences. 2016; 13: 8–18.

[12] Huang H, Lu Q, Ye C, Wei M, Yang C, Zhang L, *et al*. TAZ promotes osteogenic differentiation of mesenchymal stem cells line C3H10T1/2, murine multi-lineage cells lines C2C12, and MEFs induced by BMP9. Cell Death Discovery. 2022; 8: 499.

[13] Wang N, Liu W, Tan T, Dong CQ, Lin DY, Zhao J, *et al*. Notch signaling negatively regulates BMP9-induced osteogenic differentiation of mesenchymal progenitor cells by inhibiting JunB expression. Oncotarget. 2017; 8: 109661–109674.

[14] Wu JQ, Mao LB, Liu LF, Li YM, Wu J, Yao J, *et al*. Identification of key genes and pathways of BMP-9-induced osteogenic differentiation of mesenchymal stem cells by integrated bioinformatics analysis. Journal of Orthopaedic Surgery and Research. 2021; 16: 273.

[15] Liao J, Yu X, Hu X, Fan J, Wang J, Zhang Z, *et al*. lncRNA H19 mediates BMP9-induced osteogenic differentiation of mesenchymal stem cells (MSCs) through Notch signaling. Oncotarget. 2017; 8: 53581–53601.

[16] Dai Z, Li Y, Yan Y, Wan R, Ran Q, Lu W, *et al*. Evaluation of the internal fixation effect of nano-calcium-deficient hydroxyapatite/poly-amino acid composite screws for intraarticular fractures in rabbits. International Journal of Nanomedicine. 2018; 6625–6636.

[17] Bjelić D, Finšgar M. The Role of Growth Factors in Bioactive Coatings. Pharmaceutics. 2021; 13: 1083.
[18] Park S, Rahaman KA, Kim YC, Jeon H, Han HS. Fostering tissue engineering and regenerative medicine to treat musculoskeletal disorders in bone and muscle. Bioactive Materials. 2024; 40: 345–365.
[19] Gritsch L, Maqbool M, Mouriño V, Ciraldo FE, Cresswell M, Jackson PR, *et al*. Chitosan/hydroxyapatite composite bone tissue engineering scaffolds with dual and decoupled therapeutic ion delivery: copper and strontium. Journal of Materials Chemistry. B. 2019; 7: 6109–6124.
[20] Lee CS, Hwang HS, Kim S, Fan J, Aghaloo T, Lee M. Inspired by nature: facile design of nanoclay-organic hydrogel bone sealant with multifunctional properties for robust bone regeneration. Advanced Functional Materials. 2020; 30: 2003717.
[21] Dai Z, Li Y, Lu W, Jiang D, Li H, Yan Y, *et al*. In vivo biocompatibility of new nano-calcium-deficient hydroxyapatite/poly-amino acid complex biomaterials. International Journal of Nanomedicine. 2015; 10: 6303–6316.
[22] Dai Z, Li Y, Yan Y, Wan R, Ran Q, Lu W, *et al*. Evaluation of the internal fixation effect of nano-calcium-deficient hydroxyapatite/poly-amino acid composite screws for intraarticular fractures in rabbits. International Journal of Nanomedicine. 2018; 13: 6625–6636.
[23] Safari B, Davaran S, Aghanejad A. Osteogenic potential of the growth factors and bioactive molecules in bone regeneration. International Journal of Biological Macromolecules. 2021; 175: 544–557.
[24] Hu C, Ashok D, Nisbet DR, Gautam V. Bioinspired surface modification of orthopedic implants for bone tissue engineering. Biomaterials. 2019; 219: 119366.
[25] Luu HH, Song WX, Luo X, Manning D, Luo J, Deng ZL, *et al*. Distinct roles of bone morphogenetic proteins in osteogenic differentiation of mesenchymal stem cells. Journal of Orthopaedic Research: Official Publication of the Orthopaedic Research Society. 2007; 25: 665–677.
[26] Kim S, Cui ZK, Kim PJ, Jung LY, Lee M. Design of hydrogels to stabilize and enhance bone morphogenetic protein activity by heparin mimetics. Acta Biomaterialia. 2018; 72: 45–54.
[27] Clabaut A, Grare C, Rolland-Valognes G, Letarouilly JG, Bourrier C, Andersen TL, *et al*. Adipocyte-induced transdifferentiation of osteoblasts and its potential role in age-related bone loss. PloS One. 2021; 16: e0245014.
[28] Zhang X, Liu T, Ran C, Wang W, Piao F, Yang J, *et al*. Immunoregulatory paracrine effect of mesenchymal stem cells and mechanism in the treatment of osteoarthritis. Frontiers in Cell and Developmental Biology. 2024; 12: 1411507.
[29] Grgurevic L, Pecina M, Vukicevic S. Marshall R. Urist and the discovery of bone morphogenetic proteins. International Orthopaedics. 2017; 41: 1065–1069.
[30] Sreekumar V, Aspera-Werz RH, Tendulkar G, Reumann MK, Freude T, Breitkopf-Heinlein K, *et al*. BMP9 a possible alternative drug for the recently withdrawn BMP7? New perspectives for (re-)implementation by personalized medicine. Archives of Toxicology. 2017; 91: 1353–1366.
[31] Fujioka-Kobayashi M, Sawada K, Kobayashi E, Schaller B, Zhang Y, Miron RJ. Osteogenic potential of rhBMP9 combined with a bovine-derived natural bone mineral scaffold compared to rhBMP2. Clinical Oral Implants Research. 2017; 28: 381–387.
[32] Wang X, Chen W, Chen Z, Li Y, Wu K, Song Y. Preparation of 3D Printing PLGA Scaffold with BMP-9 and P-15 Peptide Hydrogel and Its Application in the Treatment of Bone Defects in Rabbits. Contrast Media & Molecular Imaging. 2022; 2022: 1081957.
[33] Shi P, Zhou W, Dong J, Li S, Lv P, Liu C. Scaffolds of bioactive glass (Bioglass®) combined with recombinant human bone morphogenetic protein -9 (rhBMP-9) for tooth extraction site preservation. Heliyon. 2022; 8: e08796.
[34] Sherafati Chaleshtori A, Marzhoseyni Z, Saeedi N, Azar Bahadori R, Mollazadeh S, Pourghadamyari H, *et al*. Gelatin-based nanoparticles and antibiotics: a new therapeutic approach for osteomyelitis? Frontiers in Molecular Biosciences. 2024; 11: 1412325.
[35] Li S, Yuan H, Pan J, Fan W, Zhu L, Yan Z, *et al*. Correction: The treatment of femoral neck fracture using VEGF-loaded nanographene coated internal fixation screws. PloS One. 2018; 13: e0191143.
[36] Sheikh Z, Najeeb S, Khurshid Z, Verma V, Rashid H, Glogauer M. Biodegradable Materials for Bone Repair and Tissue Engineering Applications. Materials (Basel, Switzerland). 2015; 8: 5744–5794.
[37] Kaya İ, Şahin MC, Cingöz İD, Aydın N, Atar M, Kızmazoğlu C, *et al*. Three Dimensional Printing and Biomaterials in the Repairment of Bone Defects; Hydroxyapatite PLA Filaments. Turkish Journal of Medical Sciences. 2019; 49: 922–927.